Thermochimica Acta, 61 (1983) 319–327
Elsevier Scientific Publishing Company, Amsterdam – Printed in The Netherlands

THE RECONSTRUCTIVE DECOMPOSITION OF TIN(II) FORMATE IN OXIDISING AND INERT ATMOSPHERES

J. FENERTY, P.G. HUMPHRIES and J. PEARCE

Department of Chemistry and Biochemistry, Liverpool Polytechnic, Liverpool L3 3AF (Gt. Britain)

(Received 9 August 1982)

ABSTRACT

A reaction sequence has been proposed for the decomposition of tin(II) formate in oxidising and inert atmospheres by an endothermic reaction to give tin(II) oxide. Double endothermic peaks at 473 and 483 K were ascribed to decomposition and decomposition/melting of the formate. The possibility of carbonate formation during formate decomposition was discounted on experimental evidence. At 827 K, disproportionation of the tin(II) oxide occurred exothermically with metallic tin, produced as the result of disproportionation, being rapidly oxidised in both air and "oxygen-free" nitrogen. The disproportionation of tin(II) oxide in nitrogen and argon occurred at 813 and 815 K, respectively. Oxidation of metallic tin did not occur in argon atmosphere. Scanning electron micrographs (SEM) suggested that the growth of tin(II) oxide particles formed in the decomposition was equienergetic in all directions, indicating the decomposition to be of a reconstructive nature. Non-isothermal decomposition studies did not provide consistent reaction orders but rather indicated that the data fitted different orders equally well.

INTRODUCTION

Tin(II) oxysalts decompose in air to give tin(IV) oxide when the anion is a weak electron donor, such as sulphate [1], and tin(II) oxide when the anion is a strong electron donor, such as formate [1]. Acceptor–donor character is of use in predicting whether basic or complex salt formation will occur. For the case of a weak donor, such as sulphate, the basic salt may be formed, but for an anion of strong donor ability, such as formate, no basic phase occurs and complex formation is possible. When tin(II) oxide is the reaction product, a disproportionation to give tin(IV) oxide and metallic tin occurs at higher temperatures. Metallic tin formed as a result of disproportionation is readily oxidised to tin(IV) oxide. This reaction sequence has been variously reported, with intermediate oxides postulated [2–4].

In the solid state, decomposition takes place within a restricted reaction zone [5], forming an interface between reactant and solid product. The growth of the reactant/product interface is complex and many equations

0040-6031/83/0000–0000/$03.00

have been developed to describe the overall rate process and relate it to the kinetics of decomposition [6]. Kinetic data can be obtained by an isothermal method in which the rate constants obtained over a narrow range of fixed temperatures may be used to evaluate Arrhenius parameters [7]. An alternative method of evaluating Arrhenius parameters is the non-isothermal or rising-temperature approach [8]. There are two methods within this approach by which the Arrhenius parameters may be established: (i) the differential method and (ii) the integral method. Within these two classifications there are many variations [9–11]. In this study, one example of each method has been applied [12,13]. The significance of data derived from rising-temperature kinetic studies has been the subject of much criticism [14,15], but is widely used since the Arrhenius parameters may, in theory, be derived from a single thermogravimetric experiment.

EXPERIMENTAL

Material

Tin(II) formate was prepared and its purity confirmed by quantitative chemical analysis, X-ray powder diffraction and infrared spectroscopy [16–18]. Samples were stored in a desiccator under an atmosphere of dry nitrogen prior to use.

Apparatus

Thermal work was carried out using a DuPont 990 Thermal Analyser system comprising a 951 TG and a 910 DTA cell base.

Samples were decomposed in air, white spot nitrogen and argon (250 cm^3 min^{-1}) at a heating rate 2°C min^{-1}.

Low-temperature nitrogen adsorption data was acquired using a Micromeritics model 2100D Orr Physical Adsorption Analyser. Surface areas were calculated using the BET method.

A Willis Miran 104/1A–CVF variable path length infrared gas analyser was used to identify gaseous reaction product.

The X-ray powder diffraction patterns of samples were taken by an A.E.I. Raymax unit and Van Arkel camera using nickel filtered CuK_α radiation over a 90 min exposure period.

Scanning electron microscopy (SEM) was carried out on a Cambridge Stereoscan 54 electron microscope.

RESULTS

The DTA traces obtained are shown in Fig. 1 together with the DTA of tin powder (350–450 BSS mesh) under the same conditions. The decomposition of the tin(II) formate gave a double endotherm at 473 and 483 K in both oxidising and inert atmospheres with a mass loss of 35.4%, corre-

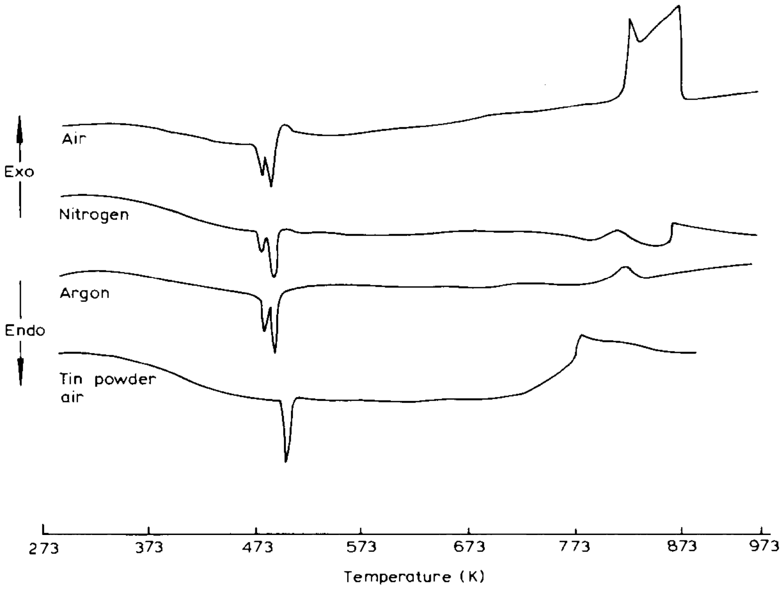

Fig. 1. DTA of tin(II) formate in oxidising and reducing atmospheres.

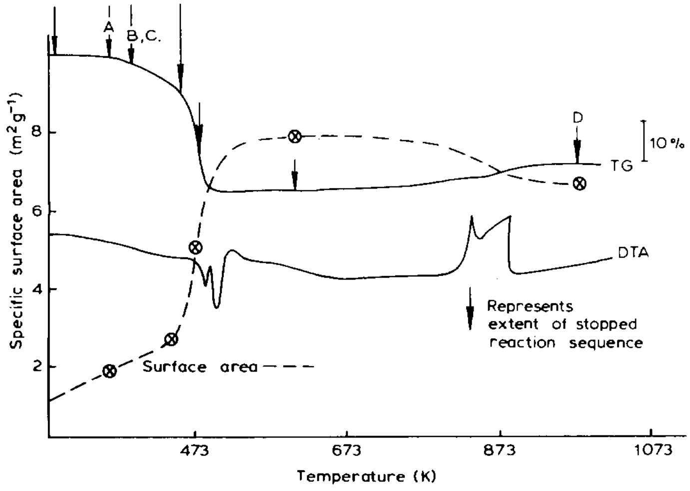

Fig. 2. Thermal analysis of tin(II) formate in air. A, B, C, D correspond to the points at which scanning electron micrographs were taken of the samples from the stopped-reaction sequence [see Fig. 3(A)–(D)].

sponding to the formation of tin(II) oxide. This was confirmed by X-ray powder diffraction.

In air, a distinctive exotherm occurred at 827 K with a sudden cut-off at 873 K. In nitrogen and argon, the exotherm occurred at lower temperatures, viz. 813 and 815 K, respectively.

The decomposition of tin(II) formate in air was followed by scanning electron microscopy (SEM) and low-temperature nitrogen adsorption techniques by employing a stopped-reaction sequence (Fig. 2). In the early stages of the decomposition ($\alpha = 0.063$), SEM indicated tin(II) oxide growth nuclei as "cabbage-like" structures with the diameter of 5–8 μm [Fig. 3(A)]. Growth of these structures continued during decomposition until, at $\alpha = 1.0$, they were 30–55 μm in diameter [Fig. 3(B), (C)]. The electron micrographs also indicated a change in particulate character during the decomposition, from the coarse particles of formate to the finer oxide particles. This change in particulate character was indicated by a sharpening and broadening of the X-ray diffraction lines and by an increase in specific surface areas (Fig. 2). A decrease in specific surface area above 673 K was consistent with the sintering of oxide particles [Fig. 3(D)].

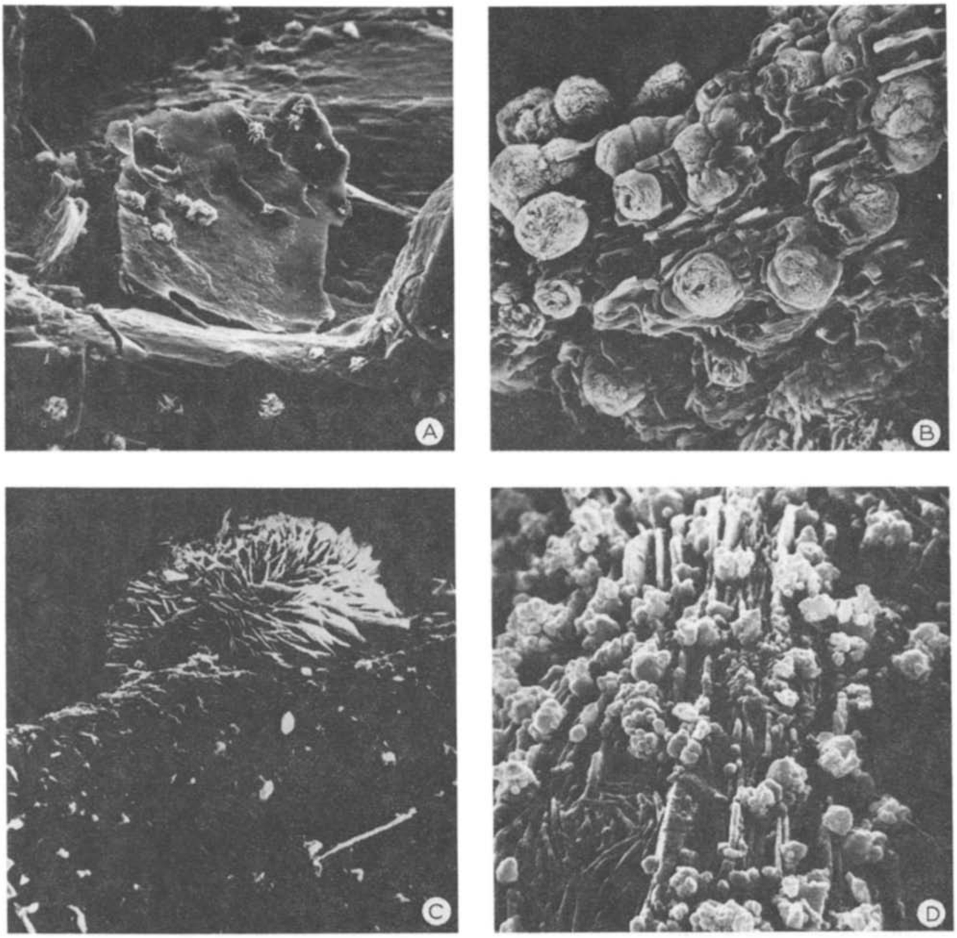

Fig. 3. Scanning electron micrographs of decomposition residues taken from the tin(II) formate decomposition at points A–D (see Fig. 2). A, $\alpha = 0.063$, ×1000; B, $\alpha = 0.258$, ×500; C, $\alpha = 0.258$, ×2000; D, $\alpha = 1.00$, temperature extent = 963 K, ×5000.

DISCUSSION

The double endotherm occurring in the decomposition of tin(II) formate in both oxidising and inert atmospheres suggested that carbonate formation was a possibility in the reaction sequence

$$Sn(HCOO)_2 \rightarrow SnCO_3 + H_2CO \quad (1)$$

$$SnCO_3 \rightarrow SnO + CO_2 \quad (2)$$

X-Ray powder diffraction photography showed no evidence of carbonate formation and further indicated that tin(II) oxide was the sole crystalline product prior to the second endotherm. Infrared analysis of the evolved gases confirmed that carbon dioxide and methanal were both evolved from the commencement of reaction and not consecutively as reactions (1) and (2) would require. Further studies, including hot stage microscopy and reflected light intensity measurements, indicated a melting of the formate marginally above its decomposition temperature when the heating rate was in excess of 0.5° $\min^{-1}$. This phenomena would attribute the second endotherm to a combined melting and decomposition [19]. The sharp single endotherm at 504 K for the powdered tin sample was due to the melting of the metal.

The exothermic peak in air at 827 K, with its sudden cut-off at 873 K, appears to be due to disproportionation of the tin(II) oxide and the almost simultaneous oxidation of liquid tin metal product to tin(IV) oxide. This oxidation occurs at 777 K (Fig. 1) when tin powder is heated at the same temperature program. The sudden cut-off in the endothermic peak at 873 K was attributed to the accelerated oxidation of tin metal, which was produced above its decomposition temperature, conditions which caused an abrupt disappearance of the metal so formed. The disproportionation of tin(II) oxide produced as the result of formate decomposition in "oxygen-free" nitrogen occurred at 813 K. The subsequent immediate oxidation of the metallic tin produced was again evident, indicating the sensitivity of the system to oxidation. The exotherm at 815 K in argon atmosphere was due to disproportionation alone; oxidation of the tin metal produced in this instance did not occur. The presence of tin metal was verified by the presence of the fusion peak for tin on the DTA cooling cycle and by X-ray powder diffraction, which indicated lines attributable to tin(IV) oxide and tin metal only. Below 815 K, the decomposition of tin(II) formate in argon produced only tin(II) oxide.

Although no intermediate oxides were detected by X-ray powder diffraction photographs on solid residues taken from the stopped-reaction sequence, it was evident from the TG recorded in air (Fig. 2), that a mass gain of 1.6% occurred up to 773 K. In contrast, the TG of metallic tin, under the same conditions, showed a mass gain commencing at 773 K. It would appear, then, that tin(II) oxide is slowly oxidised over a wide temperature range before its disproportionation at temperatures in excess of 773 K.

The reaction sequence for tin(II) formate decomposition may be represented as

$$Sn(HCOO)_2 \rightarrow SnO + CO_2 + H_2CO \quad (3)$$

$$SnO + \tfrac{1}{2}\,O_2 \rightarrow SnO_2 \quad (4)$$

$$2\,SnO \rightarrow Sn + SnO_2 \quad (5)$$

$$Sn + O_2 \rightarrow SnO_2 \quad (6)$$

Reactions (4) and (6) only occur in oxidising atmospheres.

The stopped-reaction sequence (Fig. 2) provided residues which enabled the above reactions to be followed. The overall hemispherical growth of nuclei observed in the electron micrographs suggested that the growth of tin(II) oxide [reaction (3)] was equienergetic in all directions, indicating the decomposition to be of a reconstructive nature. The disproportionation [reaction (5)] and oxidation reactions [reactions (4) and (6)] were followed by the SEM technique. Metallic tin, formed as the result of disproportionation, appeared as globules on the surface of the oxide matrix before being oxidised to tin(IV) oxide. The tin(IV) oxide formed in this way appeared as spots in the electron micrograph [Fig. 3(D)]. Oxidation and sintering of the "cabbage-like" tin(II) oxide structures prior to disproportionation was also indicated by the electron micrographs and by a consequent decrease in specific surface area (Fig. 2). Complete nitrogen adsorption isotherms on both the formate and the oxide residues were concave with respect to the pressure axis throughout the entire pressure range (Type B/Y of the Dollimore et al. classification [20]). This is consistent with a situation in which adsorbate–adsorbate interactions feature dominantly in the adsorption process and suggests that the external surface is the major factor in the physical form of the solid.

Kinetic parameters have been estimated for reaction (3) by non-isothermal methods. The integral method of Coates and Redfern [12]

$$\ln\left(\frac{1-(1-\alpha)^{1-n}}{T^2(1-n)}\right) = \ln\frac{AR}{\beta E}\left(1-\frac{2RT}{E}\right) - \frac{E}{RT} \quad (7)$$

where E is the activation energy, A the pre-exponential factor and β the heating rate, and the differential approach of Dollimore et al. [13]

$$\ln\left[\frac{d\alpha/dT}{F(\alpha)}\right]\beta = \ln A - \frac{E}{RT} \quad (8)$$

were applied for various orders of reaction (n). Table 1 indicates the orders selected, together with the integral and differential forms of $F(\alpha)$. A Fortran program was used to calculate the differential of α with respect to temperature (T) using Savitzky and Golay's method [21]. The program output consisted of a series of pseudo-Arrhenius plots in which the linear regions were selected and linear regression applied. For each approach, the "best fit"

TABLE 1

Order type functions for non-isothermal kinetics

Reaction order n	Function $F(\alpha)$	
	Integral form	Differential form
0	$Kt = 1-(1-\alpha)$	
1	$Kt = -\ln(1-\alpha)$	$\mathrm{d}\alpha/\mathrm{d}t = K(1-\alpha)$
2	$Kt = (1-\alpha)^{-1}$	$\mathrm{d}\alpha/\mathrm{d}t = K(1-\alpha)^2$
1/3	$Kt = 1-(1-\alpha)^{2/3}$	$\mathrm{d}\alpha/\mathrm{d}t = 1/2K(1-\alpha)^{1/3}$
1/2	$Kt = 1-(1-\alpha)^{1/2}$	$\mathrm{d}\alpha/\mathrm{d}t = 2K(1-\alpha)^{1/2}$
2/3	$Kt = 1-(1-\alpha)^{1/3}$	$\mathrm{d}\alpha/\mathrm{d}t = 3K(1-\alpha)^{2/3}$

regions were selected using the t-test. The reaction order was also estimated by Doyle and Slade's method [22]. Two distinct linear regions, corresponding to low and high α, were obtained with the change in slope occurring at about $\alpha = 0.37$. SEM indicated that, at this point, a situation corresponding to the overlap of growth nuclei existed. No consistent reaction order was established from the two mathematical approaches, in fact different orders

TABLE 2

Arrhenius parameters from non-isothermal calculations

Ref.	E_a (kJ mole^{-1})	t stat	$\ln A$	t stat	n
Low α					
13	59.4[a]	71.4	9.4	40.8	1
	59.9[a]	71.4	9.0	39.1	1/3
	53.5	50.0	7.5	24.2	2
	51.5	43.5	5.0	15.6	2/3
	50.7	38.5	6.9	18.9	2
12	74.0	31.2			1/2
	59.8	58.8			2
	49.0	58.8			2/3
	68.9	50.0			2
High α					
13	193.0	47.6	44.2	8.3	2
	221.5[a]	47.6	49.4	41.8	1
	221.4[a]	47.6	48.9	41.5	1/3
	175.6	25.6	38.9	22.2	1
	175.6	25.6	38.5	22.0	1/3
12	117.8	13.9			1/3
	146.5	13.5			1

[a] Indistinguishable pairs of values from one experiment.

appeared to fit the data equally well, although Doyle and Slade's method always described the reaction as first order.

Tabulation of the Arrhenius parameters in Table 2 indicates that values of activation energy and pre-exponential factor were not reproducible. Some correlation does exist within each method, the correlation being better for the differential method than the integral approach. Curiously, it was found that a linear compensation plot was obtained for the differential results. A compensation plot was not possible for the integral method since discrete pre-exponential factors (A) are not obtainable by this approach. The relationship between activation energy (E_A) and pre-exponential factor (A) for the differential method was found to be

$$E_A = m \ln A + C \tag{9}$$

for which low α gave $m = 2171.5$ and $C = 38583$, and high α gave $m = 4366.0$ and $C = 5401.4$.

It would appear from this work and elsewhere [14,23] that there are many problems to be overcome in the application of non-isothermal kinetics to heterogeneous decompositions. At present we feel we can only give an indication of activation energy and pre-exponential factors for the decomposition described here.

REFERENCES

1 J.D. Donaldson and W. Moser, J. Chem. Soc., (1960) 4000.
2 F. Lawson, Nature (London), 215 (1967) 955.
3 B.A. Kostanyan, D.A. Gedakyan, S.A. Babayan and L.G. Unanyan, Invest. Akad. Nauk SSSR Neorg. Mater., 9 (1973) 1327.
4 Z.P. Titoya, E.V. Savina and D.N. Kloshin, Zh. Prikl. Khim., 37 (1964) 2150.
5 F. Paulik and J. Paulik, J. Therm. Anal., 5 (1973) 253.
6 P.W.M. Jacobs and F.C. Tomkins, Chemistry of the Solid State, Butterworths, London, 1955, Chap. 7.
7 C.J. Keatch and D. Dollimore, An Introduction to Thermogravimetry, Heyden, London, 1975.
8 M.E. Brown, D. Dollimore and A.K. Galwey, in C.H. Bamford and C.F.H. Tipper (Eds.), Comprehensive Chemical Kinetics, Vol. 22, Elsevier, Amsterdam, 1980.
9 I. Agherglinei, J. Therm. Anal., 17 (1979) 191.
10 A.I. Chizlik, Vysokmol. Soedin. Ser A., 21 (1979) 1674.
11 H.H. Horowitz and G. Metzger, Anal. Chem., 35 (1963) 1465.
12 A.W. Coates and J.P. Redfern, Nature (London), 201 (1964) 68.
13 D. Dollimore, G.R. Heal and B.W. Krupay, Thermochim. Acta, 24 (1978) 293.
14 T.B. Tang and M.M. Chaudhri, J. Therm. Anal., 18 (1980) 247.
15 J. Leyho, M. Macnejewski and R. Szuniewicz, J. Therm. Anal., 17 (1979) 263.
16 J.D. Donaldson and J.F. Knifton, J. Chem. Soc., (1964) 4801.
17 P.G. Harrison and E.W. Thornton, J. Chem. Soc. Dalton Trans., 10 (1978) 1274.
18 J.D. Donaldson and W. Moser, Analyst, 84 (1959) 10.
19 J. Fenerty, P.G. Humphries and J. Pearce, to be published.
20 D. Dollimore, P. Spooner and A. Turner, Surf. Technol., 4 (1976) 121.

21 A. Savitzky and M.J.E. Golay, Anal. Chem., 36 (1964) 1627.
22 C.D. Doyle and P.E. Slade, Techniques and Methods of Polymer Evaluation, Vol. 6, Arnold, London, 1966, p. 113.
23 I.V. Arkhangel'skii, L.N. Komissarova and N.A. Chernova, J. Therm. Anal., (1980) 347.